Lawrence Berkeley Laboratory
UNIVERSITY OF CALIFORNIA

Physics, Computer Science & Mathematics Division

Submitted for publication

A NOVEL APPROACH TO SOLVING NON-STEADY REACTIVE GAS FLOWS

John Kurylo

September 1979

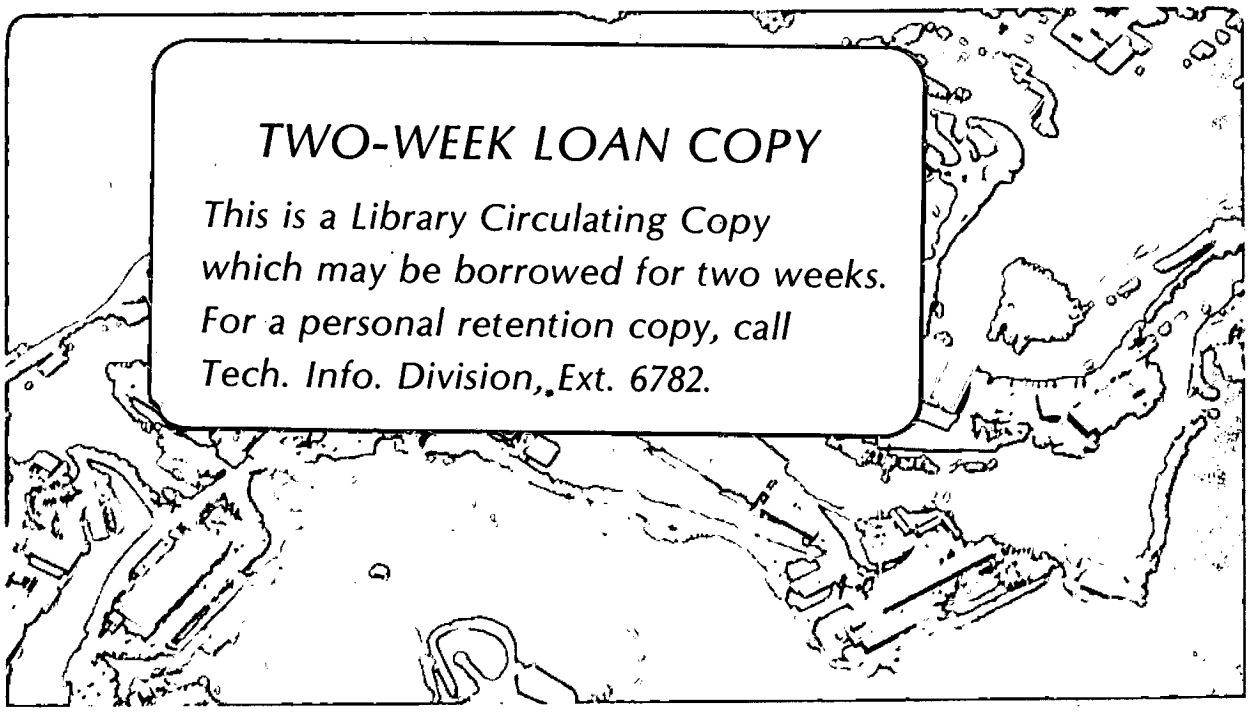

Prepared for the U.S. Department of Energy under Contract W-7405-ENG-48

DISCLAIMER

A NOVEL APPROACH TO SOLVING NON-STEADY REACTIVE GAS FLOWS

Number of pages: 33 + Figure Captions + v

Number of figures: 11 (number 1 through 10)

Number of tables: 2

Running head: A Novel Approach-Reacting Gas Flows

Send proofs to: John Kurylo
Physics, Computer Science and Mathematics Division
Building 50A, Room 2117
Lawrence Berkeley Laboratory

TABLE OF CONTENTS

LIST OF SYMBOLS

b	lower case latin "bee"
c_p	lower case latin "cee" subscript lower case latin "pee"
f	lower case latin "eff"
h	lower case latin "aytch"
i	lower case latin "eye"
n	lower case latin "enn"
o	lower case latin "oh"
p	lower case latin "pee"
r	lower case latin "arr"
t	lower case latin "tee"
t'	lower case latin "tee" superscript prime
u	lower case latin "eu"
x	lower case latin "x"
x'	lower case latin "x" superscript prime
x_f	lower case latin "x" subscript lower case latin "eff"
A	upper case latin "Ay"
A^A	upper case latin "Ay" superscript upper case latin "Ay"
E	upper case latin "E"
K	upper case latin "Kay"
K_o	upper case latin "Kay" subscript lower case latin "oh"
L	upper case latin "ell"
N	upper case latin "enn"
N_{Da_o}	upper case latin "enn" subscript upper case latin "Dee" lower case latin "ay" subscripted by lower case latin "oh"

Q	upper case latin "que"
$\dot{Q}$	upper case latin "que" with dot over center of "que"
R	upper case latin "arr"
S	upper case latin "ess"
S'	upper case latin "ess" superscript prime
T	upper case latin "Tee"
T_o'	upper case latin "Tee" superscript prime subscript lower case latin "oh"
T_i^{n+1}	upper case latin "Tee" superscript lower case latin "enn" plus one, subscript lower case latin "eye"
$T(x)$	upper case latin "Tee", open paren, lower case latin "x", close paren
T_{max}	upper case latin "tee" subscript "max"
Z	upper case latin "Zee"
$\dot{Z}$	upper case latin "Zee" with dot over center of "Zee"
Z_i^n	upper case latin "Zee" superscript lower case "enn", subscript
i	lower case latin "eye"
α	lower case greek "alpha"
δ	lower case greek "delta"
δ'	lower case greek "delta" superscript prime
ε	lower case greek "epsilon"
λ	lower case greek "lamda"
π	lower case greek "pi"
ρ	lower case greek "rho"
σ	lower case greek "sigma"
τ	lower case greek "tau"

τ'	lower case greek "tau" superscript prime
τ_i	lower case greek "tau" subscript lower case latin "eye"
Δ	upper case greek "delta"
Δh	upper case greek "delta," lower case latin "aytch"
$\Delta x'$	upper case greek "delta," lower case latin "x" with superscript prime
Δt_p^n	upper case greek "delta," lower case latin "tee" with superscript lower case latin "enn" and subscript lower case latin "pee"
$\frac{\partial}{\partial}$	1st partial derivative symbol
$\frac{\partial^2}{\partial}$	2nd partial deviation symbol
$\frac{d}{d}$	1st ordinary derivative symbol
e	exponential symbol ex. $e^{-E/RT}$
0	zero
1/2	one half
1	one
$\leqslant$	less than and equal to symbol
>	greater than symbol
=	equal to symbol
( )	paren symbol
/	divide symbol ex. w/2 lower case latin "double-eu" divided by two
$+\infty$	plus infinity symbol

$\lvert\ \rvert$	absolute value symbol
$\sqrt{\ }$	square root symbol
ln	natural logarithm symbol

A NOVEL APPROACH TO SOLVING NON-STEADY REACTIVE GAS FLOWS

John Kurylo

Physics, Computer Sciences and Mathematics
Lawrence Berkeley Laboratory
University of California
Berkeley, CA 94720

ABSTRACT

A novel numerical technique for the efficient solution of the model equations describing reactive gas flows is presented. This technique models the combustion process as a deflagration working inconjunction with a flame dictionary. The entries in the dictionary constitute a compendium of steady-state flame solutions under the gasdynamic and chemical conditions encountered by the flame as it progresses through the flow field. Each entry is the result of a fine-scale numerical calculation. This technique overcomes the numerical problems associated with the multiple length and time scales characteristic of reacting gas flows. Numerical experiments illustrate that the dictionary technique represents a significant improvement over conventional finite-difference approaches.

INTRODUCTION

Over the last few decades, time-dependent gas flows have increasingly been analyzed by numerical methods. This dependence on numerical methods stems from: the ever-increasing costs and complexity of physical experimentation; the inability of analytic approaches to handle the model's systems of nonlinear partial and ordinary differential equations; the analyst's desire to incorporate into the model the complete and latest details of the chemical and transport processes; the advances in computer technology (memory and speed); and the development of efficient numerical techniques which can account for irregular three-dimensional domains, turbulence, and boundary layers in the model [1-5]. As the capabilities of numerical methods to serve as a design tool and/or as a means of analyzing current practical non-steady reactive gas flows continue to expand, their cost decreases.

There are two distinct scales in reactive gas flows, one associated with the combustion front and the other with the hydrodynamic flow. Although analytic solutions describe the evolution of the flow with infinite spatial and time resolution, numerical solutions--due to practical limitations on computer memory, time, and overall expense--have traditionally been hindered by multiple length and time scales.

Pollution formulation and the wave speed of the combustion process depend on the structure of the combustion wave. Accurate predictions of combustion properties by the numerical scheme require a grid

spacing that can represent the variation of temperature and species concentration throughout the combustion wave. For hydrodynamic waves, however, wave speed can be accurately predicted independent of computed structure and only the Rankine-Hugoniot relations need be satisfied across the wave. Grid spacings can thus be several orders of magnitude larger than the wave thickness.

The conventional procedure for modeling reacting gas flows has therefore been to integrate the complex chemical reaction equations while accounting for the fluid motion, the effects of viscosity, and the diffusion of heat and species at each point in the computational grid. With a sufficiently fine grid system, this approach yields a computationally stable and accurate description of the chemical and gasdynamic states throughout the combustion wave. Since the typical flame thickness is 10^{-2} cm [6] the restriction imposed by stability and accuracy on the allowable time step used for the advancement of the flame calculations is severe, on the order of 10^{-7} seconds, making it extremely difficult to model practical reactive gas flows using conventional numerical methods. Attempts to alleviate the problem of scales have centered around variable grid techniques. However, these methods still require the continual evaluation of detailed chemistry, heat transfer, and fluid motion at each step of the calculations. Also, the time-step limitation, as noted above, applies at each step of the calculations.

The numerical technique presented in this paper recognizes the combustion event as a small entity in a vast non-reacting flow field which can thus be treated as a deflagration [7]. The novel concept is

that at each instant the deflagration characterizes one entry in a flame dictionary. Each entry in this dictionary contains detailed information about the combustion process's steady-state physical and chemical structure, flame burning speed, and flame thickness for a particular set of gasdynamic and chemical conditions. The dictionary provides the large-scale hydrodynamic calculations with the needed small-scale influence.

The paper begins by defining a model for non-steady laminar flames, and proposing a model for the nonlinear dependence of heat release rate on time. The difficulties arising from the nonlinearity and structure of the model's governing equations are discussed as are problems associated with multiple scales occurring in the flow, their effects on the modeling of practical reacting gas flows, and attempts to alleviate these problems. A discussion of the dictionary technique follows. The section on RESULTS describes the numerical techniques and conditions used to solve the model equations, and discusses the dependence of flame thickness and burning speed on the parameters in the model, the sensitivity of these properties on the grid spacing, and typical effects of insufficient flow field definition. Next, use of the dictionary technique, under conditions simulating practical reactive gas flows, is demonstrated. This includes defining the flow field and disturbance, establishing the entries for the dictionary, and testing the response of the dictionary technique to various size disturbances. Dictionary results are compared to results computed by finite-differences. The advantages and adaptability of the

dictionary technique to practical reactive gas flows are considered, in light of conclusions drawn from the results of the numerical experiments.

MODEL PROBLEM, ANALYSIS, AND METHOD OF SOLUTION

The essential features of the physical and chemical processes governing the structure and progress of premixed non-steady laminar flames are contained in the following set of model equations:

$$\text{(Energy)} \qquad \rho c_p \frac{\partial T'}{\partial t'} = \lambda \frac{\partial^2 T'}{\partial x'^2} - \rho \Delta h \dot{Z} \quad , \tag{1}$$

and

$$\text{(Reaction)} \qquad \dot{Z} = \frac{dZ}{d(t' - \tau')} = - KZ \quad , \tag{2a}$$

where

$$K = 0 \quad \text{if} \quad T' \leqslant T'_o \quad ,$$
$$K = K_o \quad \text{if} \quad T' > T'_o \quad . \tag{2b}$$

Equation (1) describes the energy balance that exists at each point in the flame between (a) the rate of change of sensible heat content of the medium, and (b) the two competing processes of net influx of heat by conduction and the rate of heat generation associated with converting reactants into products. In Eq. (1), T' represents the dependent variable temperature, $\dot{Z}$ the time rate of change of the progress parameter (reactants: Z = 1; products: Z = 0), and t' and x' the independent variables time and space, respectively. The coefficients ρ, c_p, λ, and Δh denote the participating medium's density, the specific heat at constant pressure, the coefficient of thermal conductivity, and the heat of reaction, respectively, and are

assumed to be constant. With constant coefficients, Eq. (1) models combustion in a solid medium without gas generation. It also describes combustion in a gaseous medium having a very low heat of reaction and a greater ability to diffuse heat than species (Lewis-Semenov number >> 1). In a typical gaseous combustive reaction, the coefficients are nonlinearly dependent on temperature and the Lewis-Semenov number is approximately one [6]. Assuming temperature-dependent coefficients slightly modifies the form of Eq. (1) but also reduces our ability to distinguish the role of each coefficient in the solution. So, for the present study, we extend Eq. (1) to gaseous reactions with large heat release. Equations (1), (2a), and (2b) are meant to model only the key features of typical gaseous reactions.

Equation (2a) is the reaction rate equation which Z, the progress parameter, satisfies. Equation (2b) restricts reaction to those portions of the flow field that have attained a minimum temperature of T_o'. Here K represents the reaction rate, T_o' the ignition temperature, and τ' (a dependent quantity) the instant the fluid element attains the ignition temperature. The dependence of the reaction rate on the fraction of unburned medium remaining is typical of phenomenological chemical kinetic expressions [8]. From Eqs. (2a) and (2b) the time dependence of the progress parameter and specific heat release rate, $\dot{Q}$, are found to be:

$$Z = e^{-K(t'-\tau')} \qquad Z(0) = 1 \quad , \tag{3}$$

and

$$\dot{Q} = -\Delta h\dot{Z} = (K\Delta h)\, e^{-K(t'-\tau')} \quad , \tag{4}$$

where

$$K = 0 \quad \text{if} \quad T' \leq T'_o \quad ,$$

and (2b)

$$K = K_o \quad \text{if} \quad T' > T'_o \quad .$$

Equations (3) and (4) indicate that the progress parameter and heat release-rate decay exponentially in time after the reaction starts. Conduction of heat from the higher temperature to the lower temperature portions of the flow field represents the only mechanism by which the temperature of the combustible medium can increase to the value T'_o. During this induction period the reactants undergo the build up of radicals.

Figure 1 displays the time dependence of the heat release-rate, assuming adiabatic combustion, specified by Eq. (4), a well-stirred reactor (WSR) [9], and a typical Arrhenius kinetic expression [10], i.e.,

$$\dot{Q} = Ae^{-E/RT'} \quad ,$$

where E denotes the energy of activation, R the gas constant, and A the pre-exponential factor. The heat release rate characteristics of a WSR are typical of those observed experimentally in reactive waves. In a WSR, the heat release rate experiences a smooth but rapid

increase in time (totaling 25% of the total heat released) followed by a longer period during which the remaining 75% of the heat is released. In the case of the Arrhenius expression, the rate of heat release continually rises. Equation (4) simulates the larger latter portion of the WSR's heat release-rate curve. In addition, the results of numerical calculations can be compared to the analytic solution of the steady state form of Eq. (1) for the reaction model given by Eqs. (2a) and (2b). The problems faced by the modeler in handling the heat release portion of Eq. (1) are contained in Eq. (4). The model of non-steady laminar flames defined by Eqs. (1), (2a), and (2b) includes many of the essential and important non-linearities and difficulties which confront the successful modeler. A brief discussion of these difficulties follows.

To better understand the structure of Eq. (1), we nondimensionalize the dependent and independent variables as follows [11]:

$$\Delta T'_o = \frac{\Delta h}{c_p} \quad , \quad T = \frac{T'}{\Delta T'_o} \quad , \quad T_o = \frac{T'_o}{\Delta T'_o} \quad ,$$

$$x = \frac{x'}{L} \quad , \quad t = \frac{t'}{L^2}\sigma \quad , \quad \tau = \frac{\tau'\sigma}{L^2} \quad , \tag{6}$$

and

$$\sigma = \frac{\lambda}{\rho c_p} \quad ,$$

where L represents the characteristic length scale in the flow field. From Eqs. (1), (2a), (2b), and (6) we obtain

$$\frac{\partial T}{\partial t} = \frac{\partial^2 T}{\partial x^2} + N_{Da} Z \quad , \tag{7}$$

and

$$Z = e^{-N_{Da}(t-\tau)} \quad , \tag{8a}$$

where

$$N_{Da} = 0 \qquad \text{if} \qquad T \leqslant T_o \quad ,$$

and $\tag{8b}$

$$N_{Da} = N_{Da_o} \qquad \text{if} \qquad T > T_o \quad ,$$

where $N_{Da} = KL^2/\sigma$ is the Damköhler number, a ratio of the heat release rate to the rate of heat conduction. Under typical combustion conditions N_{Da} can vary as much as 10 orders of magnitude from one side of the flame to the other side. In particular, for the model under consideration we will use $K_o = 92{,}103\ \text{sec}^{-1}$, $\sigma = 1.5\ \text{cm}^2/\text{sec}$, and $L = 1$ cm, yielding

$$N_{Da_{upstream}} = 0 \quad ,$$

and

$$N_{Da_{downstream}} = 6.14 \times 10^4 \quad .$$

This range of N_{Da} is difficult to model because: (1) the character of the model equations change, and (2) large temperature and progress parameter gradients arise in the flow field. In the upstream portion of the flame, Eq. (7) has a parabolic character, while at the point in the flow field where T equals T_o, the model equations are dominated by the character of ordinary differential equations (ODE's). Further downstream, the rates of heat production and heat transfer decrease rapidly. In general, the ODE's are best handled by Gear-Hindmarsh's stiff ODE parkage [12,13]. There are many efficient explicit and/or implicit solvers, such as Crank-Nickolson [14], for parabolic equations. Using either method alone to solve Eq. (7) omits the contribution of the other to the solution, and results in improper modeling of the combustion process. The operator-splitting technique overcomes this difficulty. Equation (7) is solved as a pair of equations

$$\text{(ODE)} \qquad \frac{\partial T}{\partial t} = N_{Da} Z \quad , \tag{9a}$$

and

$$\text{(Parabolic)} \qquad \frac{\partial T}{\partial t} = \frac{\partial^2 T}{\partial x^2} \quad . \tag{9b}$$

The time and space accuracy of the numerical scheme for the combined split equations is the same order as that for the single equation, Eq. (7). Attention must be paid to the proper matching of the boundary conditions. The complete theory of operator splitting can be found in Yanenko [15]. Note that by accounting for chemical

reactions and heat transfer in separate steps, the basic conservation laws may be violated at the end of each chemical step. This effect mainfests itself in the form of short-lived transients resulting in unwanted oscillations and waves. The situation is remedied by taking time-steps small enough so that all changes occur gradually. In the computations, the maximum temperature change occurring at any point in the flow field due to heat release is restricted to $5^{o}K$. This is a costly remedy to the problem of operator splitting.

The second difficulty addresses the problem of obtaining sufficient flow field definition using a difference grid. The region over which significant changes in temperature and progress parameter occur defines the flame thickness. At 10 atmospheres, hydrocarbon-air flames have a flame thickness, δ', on the order of 10^{-2} cm [6]. Adequate definition of the preheating and heat liberation zones requires a grid spacing, $\Delta x'$, at least an order of magnitude finer than the flame thickness, i.e.,

$$R = \frac{\Delta x'}{\delta'} \leqslant 0.1 \quad .$$

Larger grid spacings reduce the maximum possible gradient within the flame, altering the flame's structure and structure-dependent phenomena such as pollution formation and burning speed. The section on RESULTS clearly demonstrates the sensitivity of the numerical solution on the grid spacing used.

This grid-spacing requirement imposes an intolerable restriction on modeling practical reactive gas flows. With typical engine

cylinder dimensions being 9.53 cm in stroke by 9.86 cm in bore (compression ratio 8:1), and with a grid spacing of 0.18 cm (60 grid points in the cylinder axis direction), approximately 150,000 grid points are required to describe the cylinder volume. Yet in this case R equals 18. Approximately 8×10^{11} equally spaced grid points are required to adequately (minimally) describe flame propagation within this cylinder. Stability, accuracy, and operator-splitting considerations further worsen the situation by imposing a 10^{-7} second maximum allowable cycle-to-cycle time step. Clearly, modeling practical reactive gas flows using conventional numerical techniques is hopeless.

One of the most successful techniques to alleviate this problem is regriding [11], in which the distribution of grid points within the flow field is a dynamic process whose distribution properties depend directly on some specified quantity within the flow field, such as temperature gradient. In this case more grid points are concentrated in the regions of large temperature gradient than elsewhere. This technique uses a uniform grid spacing in the transformed space coordinate and the flame overcomes grid points slowly, allowing the modeler to use many efficient schemes for calculating parabolic flows. The slowly varying conditions at each grid point allow the calculations to proceed in an approximate steady-state manner. However, at each instant detailed calculations of chemistry, heat transfer, and fluid mechanics must be carried out. In the extreme case of a constant velocity flame propagating down an infinite tube,

these calculations become redundant and repetitive. There is always a continuous succession of grid points through the flame, and a grid point continually changes from representing conditions upstream to representing those downstream of the flame. The tremendous effort to continually calculate the flame's future progress is unnecessary once its structure and burning speed are known, since these factors remain invariant.

All this led to the idea of using a dictionary to solve problems of modeling non-steady reactive gas flows. Each entry in the dictionary contains detailed information on the combustion front's steady-state physical and chemical structure, its propagation velocity, and any other information desired for a particular set of gasdynamic and chemical conditions. The dictionary accounts for the varying conditions the flame encounters as it progresses through the flow field. Each entry is a result of a finite-difference computation using a fine grid spacing. All the difficulties associated with performing these computations will of course be encountered, but only once. The dictionary does not contain these computations, but only the results. In conjunction with the use of a dictionary, the combustion front is treated as a deflagration [7], that is, a discontinuity in the flow field across which step changes in state occur. At each instant the deflagration characterizes one entry in the dictionary.

The procedure for calculating the flow field using the dictionary technique is:

- Calculate the fluid motion and heat transfer throughout the flow field;
- Find the entry in the dictionary with conditions most similar to those immediately ahead of the deflagration;
- Transport the deflagration according to the flame burning speed.

In the extreme case of a constant velocity flame propagating down an infinite tube, the dictionary would consist of only one entry containing the structure and flame burning speed of a steady flame propagating into the gas medium in the tube. At each cycle of the numerical scheme, the same entry would be quizzed. With more complicated flows, the number of entries increases. The actual number of entries depends on the influence of the disturbance upstream of the flame on the characteristics of interest, such as flame burning speed and pollution. An example showing how to use the dictionary and its advantages over a finite-difference approach in the case of a reactive gas flow is presented in the last section of this paper.

RESULTS

The model equations, Eqs. (7), (8a), and (8b), are solved for the following condition (typical of hydrocarbon-air combustion [9]):

$$\Delta T'_o = \frac{\Delta h}{c_p} = 2000^oK \quad , \tag{10a}$$

$$N_{Da_o} = 6.14E{+}04 \quad \begin{cases} \sigma = 1.5 \text{ cm}^2/\text{sec} \\ K_o = 92{,}103 \text{ sec}^{-1} \end{cases} (Z=0.1 \text{ when } t-\tau=0.75E{-}04) \quad , \tag{10b}$$

and

$$T'_o = 1000^oK \quad . \tag{10c}$$

Boundary Conditions: $\frac{\partial T}{\partial x} = 0 \quad \text{at} \quad x = 0 \quad ,$ (11a)

$$T = T_u \quad \text{at} \quad x = +\infty \quad . \tag{11b}$$

In the calculations, the temperature boundary condition is satisfied by ensuring that at least 3 grid points are at the unburned temperature T_u. The numerical scheme used to integrate the model equations is

$$\text{(ODE)} \quad T_i^{n+1} = T_i^n + Z_i^n\left(1 - e^{-N_{Da_o}\Delta t^n}\right) \quad T > T_o \quad , \tag{12a}$$

where

$$Z_i^n = e^{-N_{Da_o}(t^n-\tau_i)} \qquad \tau_i = t \text{ when } T_o = T_o \quad ,$$

$$T_i^{n+1} = T_i^n \qquad T \leqslant T_o \quad , \tag{12b}$$

$$\left(\Delta t_r^n \mid \max_i |T_i^{n+1} - T_i^n| < \alpha\right) \qquad \alpha = 0.0025 \quad , \tag{12c}$$

$$\text{(Parabolic)} \quad T_i^{n+2} = T_i^{n+1} + \frac{\Delta t^n}{2\Delta x^2}\left(T_{i+1}^{n+1} - 2T_i^{n+1} + T_{i-1}^{n+1}\right) \quad , \tag{12d}$$

and

$$\Delta t_p^n = \Delta x^2/2 \quad , \tag{12e}$$

where

$$\Delta t^n = \min\left(\Delta t_r^n \ , \ 0.9\ \Delta t_p^n\right) \quad . \tag{12f}$$

An explicit scheme is used to integrate the ODE. For the parabolic equation, an explicit finite-difference scheme is used because of its simplicity and the time restrictions imposed by Eq. (12c). If in Eq. (12c), the value choosen for α is too large, the proper apportionment of the heat released by the chemical reaction to the sensible internal energy and heat transferred may not be carried out by the operator-splitting procedure.

Table I contains calculated and predicted values of the flame burning speed, S, and flame thickness, δ, for a range of values of the parameters N_{Da}, T_o, and T_u in the model. the flame thickness is the width of the region within the flame in which the temperature exceeds the undisturbed value T_u but is less than the burned temperature T_b by 0.01, where

$$T_b = T_u + 1 \quad .$$

The initial condition for all the computations was a step change in temperature from T_u to T_b. the calculations, using a grid spacing of 0.0005 (R = 0.015), were carried out until the flame propagated at a steady state. In Table I, only values of the parameters different from those of the first entry are noted. The temperature distribution within the flame and the analytic dependence of the flame burning speed and thickness on the parameters of the model are given by [16]:

$$T(x) = T_u + 1 - \frac{S^2}{N_{Da_o} + S^2} e^{\frac{N_{Da_o} x}{S}} \qquad x \leqslant 0 \quad , \tag{13a}$$

$$T(x) = T_u + \frac{N_{Da_o}}{N_{Da_o} + S^2} e^{-Sx} \qquad x \geqslant 0 \quad , \tag{13b}$$

$$S = \sqrt{\frac{1 - A}{A} N_{Da_o}} \quad (= S'L/\sigma) \quad , \tag{14}$$

and

$$\delta = [N_{Da_o} A(1 - A)]^{-1/2} \ln [100\, A^A (1 - A)^{1-A}] \quad (= \delta'/L) \quad , \tag{15}$$

where

$$A = T_o - T_u \quad .$$

These relations were obtained by using Green's functions to integrate the model equations. By comparing the calculated and predicted values, given in Table I, we conclude that this numerical method does

predict the dependence of the flame properties on the parameters. However, it is the effect of grid spacing on the calculated flame structure and burning speed which is of particular interest. Figure 2 displays these effects for the case of a steady flame propagating under the conditions given by the first entry in Table I. Similar results were obtained for other operating conditions. The vertical bars represent the range of flame thickness the flame experiences in its psuedo-steady-state mode of propagation. The effect of the grid spacing on the flame burning speed is evident even approaching the minimum grid spacing of 0.0005 ($R = 0.015$). However, the flame thickness is insensitive to values of Δx less than 0.004 ($R = 0.12$). At this critical grid spacing, only 8 grid points define the flame. At larger values of Δx, the temperature gradients which drive the flame can no longer be approximated with sufficient accuracy resulting in a linear growth of the calculated flame thickness. The flame continues to span 3 cells, irrespective of the grid spacing.

From Fig. 2 and Eqs. (14) and (15) we see that the effects of the grid spacing on the calculated flame properties are phenomenologically similar to those due to a variation in the inverse square of the reaction rate. Also, the magnitude of each effect is comparable to that resulting from a variation of any of the parameters in the model.

Temperature-space profiles corresponding to the various Δx in Fig. 2 are presented in Fig. 3. The positions of the grid points are indicated for profiles with $\Delta x \geq 0.004$ ($R \geq 0.12$). As noted previously, the flame structure remains unchanged for grid spacings

less than 0.004. However, drastic changes in the temperature distribution occur when Δx increases beyond 0.004 (R = 0.12). Most noticeable is the appearance of a peak temperature. This bulge in the temperature profile is mostly confined to the one cell in which the temperature most recently exceeded T_o. Note the few number of grid points which define the flame structure. The actual temperature gradient is so poorly represented by the computational grid that the heat evolved due to combustion is all but constrained to remain at that one node. This causes a temperature build up, which increases the rate of heat transfer to the surrounding grid points. As Δx increases, individual grid points begin to combust totally before the ignition of the next grid point. This causes an oscillation in the flame thickness. These oscillations are denoted by the verticle bars in Fig. 2. In constant pressure non-steady laminar flame calculations, this effect manifests itself in the surging of the particle velocity or, for the case of small but not sufficiently fine grid spacing, an unrealistic overshoot in the maximum particle velocity (dynamic pressure) prior to establishing steady-state flow conditions. Therefore, adequate representation of the flame can be assured only when the grid spacing is at least an order of magnitude finer than the flame thickness ($R \leq 0.1$).

Given the limitations of today's computers, this restriction on the grid spacing in relation to flame thickness in conventional numerical techniques is an insurrmountable obstacle, imposing two distinct characteristic space scales. By using the flame dictionary

in conjunction with a deflagration, the modeler can get fine-scale resolution in only the small portion of the flow field where he needs it, thus facilitating calculations in the remainder of the flow field.

To illustrate the practicality of the dictionary and to highlight its advantages over finite-difference procedures, both methods are used to solve the following problem: An initially steady propagating flame encounters a temperature varying flow field. The problem is to calculate the subsequent flow field, and the flame's burning speed history and trajectory. The effect of varying the width of the disturbance relative to the flame thickness, δ_u, is also examined. The temperature disturbance has the following form:

$$T(x) = T_u + \left(\frac{T_{max} - T_u}{2}\right) \cdot \left(1 - \cos\left[\frac{2(x - x_o)}{\varepsilon}\,\pi\right]\right) \qquad x_o \leqslant x \leqslant x_o + \varepsilon \quad ,$$

where x is the space coordinate; ε the width of the temperature disturbance; and x_o, T_u, and T_{max}, the upstream location of the disturbance, the undisturbed temperature in the flow field, and the maximum temperature in the disturbance, respectively. The flame and flow field properties used in the calculations are given by Eqs. (10a)-(10c), and

$$T_u = 0.150 \quad , \qquad T_{max} = 0.450 \quad , \qquad T_o = 0.500 \quad .$$

In the dictionary technique, the deflagration at each instant characterizes one entry in the dictionary. Therefore, in assembling

the dictionary we must account for the varying conditions the flame encounters as it progresses through the flow field.

For the flow field conditions specified above, 7 entries constitute the dictionary. Table II shows the temperature, T_i, defining each entry and the flame burning speed and thickness associated with that entry. Figures 4a and 4b display the temperature and progress parameter distributions, centered about a temperature $T_i + 1/2$ and $x = 0$, which are also included in the entry.

The data for each entry were obtained by using Eqs. (12a)-(12f) to calculate the steady state combustion wave arising from an initial temperature distribution corresponding to a step change in temperature from T_i to $T_i + 1$. These calculations used a grid spacing of 0.002 ($R = 0.06$).

These 7 entries were choosen to illustrate the solution of a practical problem using the dictionary technique, not to represent the optimal number or set of conditions for this problem. In more complicated flows, the actual number of entries should depend on the influence of the disturbance upstream of the flame on the flame characteristics of interest, such as flame trajectory or pollution formation.

The finite-difference solution is obtained by applying Eqs. (12a)-(12f) to each grid point in the flow field. The dictionary solution is obtained by applying Eqs. (12d)-(12f) at all grid points followed by the transport of the deflagration through the flow field. The deflagration progresses according to the flame burning speed

obtained from the dictionary. Information for conditions other than those exactly specified by the dictionary entry is obtained by linear interpolation from the entries closest to the existing conditions.

Two cases are considered:

Case 1. $x_f = 0.0846$ $x_o = 0.120$ $\varepsilon = 0.2$ $\varepsilon/\delta_u = 6$.

Case 2. $x_f = 0.1450$ $x_o = 0.180$ $\varepsilon = 2.0$ $\varepsilon/\delta_u = 60$.

Here x_f specifies the initial flame location.

Figure 5 shows the temperature-space profiles at various instants for Case 1, calculated by the finite-difference technique. Figures 6 and 7 display the temperature distributions at various instances calculated by the dictionary technique. The results shown in Fig. 6 account for heat transfer in the flow field on either side of the deflagration, while those shown in Fig. 7 do not. Neglecting heat transfer eliminates the finite-difference portion of the dictionary technique. This represents the most efficient (cost effective) method for calculating the progress of the flame. Included in each profile in Fig. 5 is the location of the flame, denoted by an x, as calculated by the dictionary technique ($\sigma = 0$). The extent of the flame about this position as obtained from the dictionary is indicated by vertical bars. Superimposed on each temperature profile in Figs. 6 and 7 is the flame temperature distribution obtained from the dictionary. These distributions, denoted by dashed lines, are centered about the deflagration position and a temperature $T_I + 1/2$, where T_I is the

temperature immediately ahead of the deflagration. Care was taken to ensure that these dictionary profiles merged smoothly with the remainder of the flow field.

A summary of the flame trajectories and burning speed profiles is presented in Fig. 8. The continuous lines represent the finite-difference solution while circles and dashes denote results of the dictionary technique, with σ equal to 1.5 and 0, respectively. We see that the finite-difference and dictionary (σ = 1.5) solutions agree extremely well. However, for the dictionary technique (σ = 0), the flame trajectory lags slightly behind the others during the initial phase of the temperature disturbance, preceeds them at the later stages, and eventually becomes indistinguishable from the true trajectory. The flame burning speed profile explains this behavior. Due to the lack of heat transfer from the high-temperature regions of the disturbance to the low-temperature regions, the flame initially encounters the gas medium at a temperature lower than in the other calculations. This results in a lower flame burning speed. In the high-temperature regions, the degredation of the heat content of the medium by heat transfer does not occur. Hence, the deflagration experiences in higher reactant temperature resulting in a higher flame burning speed. Then a condition similar to the initial phase occurs, yielding a lower flame burning speed. This behavior is caused by the exclusion of the heat transfer calculations in all but the flame.

By accounting for heat transfer, the peak temperature of the disturbed medium drops approximately 0.04 before being overcome by the combustion front. Such a significant change is due to the large potential for heat transfer as determined by $2\sigma (T_{max} - T_u)/\varepsilon$. However, as significant as the effect of peak temperature drop would appear to be, its effect on the flame burning speed is of short duration as compared to the whole event, and therefore minimal in terms of the trajectory error.

Therefore, we conclude that there is no difference between the finite-difference solution and the dictionary solution with or without σ. The finite-difference solution required a grid spacing of 0.002 and 35,806 cycles (15.8 seconds of execution on a CDC 7600) of computation, whereas the dictionary technique used a grid spacing of 0.02 and only 133 cycles (0.68 seconds) of computation, while retaining every detail of the combustion process. Perhaps even larger values of grid spacing could be successfully used.

The finite-difference technique recomputes flame structures at every instant, while the dictionary technique refers only to the results of previously calculated flame structures, representing an enormous savings in effort. The detail to which the flame can be represented is also greatly increased.

Figure 9 shows the temperature-space profiles at various instances for Case 2, calculated by both the finite-difference and the dictionary technique ($\sigma = 1.5$). The flame position calculated by the dictionary ($\sigma = 0$) is indicated by an x and the flame extent by

verticle bars. Figure 10 shows the flame trajectories and burning speed profiles (symbols as in Fig. 8). Due to the greatly increased width of the disturbance, the effect of heat transfer on the peak temperature is negligible (≤ 0.01). As in Case 1, the finite-difference and the dictionary ($\sigma = 1.5$) results are in excellent agreement, but this time the difference between these solutions and that of the dictionary ($\sigma = 0$) is completely negligible. Note that the finite-difference solution again required a grid spacing of 0.002 (1000 grid points define the temperature disturbance) and 111,530 cycles (405.2 seconds) of computation, while the dictionary technique used a grid spacing of 0.10 (20 grid points) and only 84 cycles (0.20 seconds) of computation. Perhaps even larger grid spacings could be used. The savings are tremendous.

Another example similar to Case 2, but with σ being temperature dependent, also produced very favorable results.

CONCLUSION

Finite-difference calculations carried out on equally spaced grids indicate that flame properties are strongly dependent on the grid spacing. Calculated flame burning speeds deviate from the exact value by a least 6% whenever grid spacings greater than the critical size, one order of magnitude finer than the flame thickness, are used. Flame thickness, on the other hand, is insensitive to grid spacings less than the critical size, but thereafter grows linearly with the grid spacing. The flame burning speed depends to a much greater degree on the ability of the numerical method to reproduce the maximum temperature gradient within the flame.

Deviations in flame properties due to grid spacing can be as large and even exceed the effects of variation of any of the physical parameters of the flow field. Exceeding the critical grid spacing causes bulges in the temperature profile, increases in the peak temperature, a quasi-steady oscillation in the flame thickness, oscillation in the upstream fluid velocity, and a greatly increased predicted peak particle velocity (dynamic pressure) during the initial non-steady phase of the reactive gas flow calculations.

This dependence on grid spacing should prompt the modeler to employ as fine a grid spacing as possible throughout the course of the calculations. With conventional techniques the grid requirements for accurately modeling non-steady combustion in practical devices far exceeds the resources of todays computers.

The most important feature of the dictionary technique is its ability to bridge the gap between the two characteristic space scales existing in all reacting gas flow problems. The smaller scale emerges from the modelers desire to accurately portray the structure within the flame, while the larger scale is characteristic of the remainder of the flow field. When the dictionary is coupled with a method for transporting the deflagration through the flow field, the dictionary technique becomes an extremely efficient numerical tool for calculating non-steady reactive gas flows (see Kurylo [17] for such a method.)

Once the conditions into which the deflagration propagates are determined, one simply locates which entries within the dictionary most closely resemble these operating conditions, by interpolation obtains the propagation speed and any other desireable combustion quantities, and advances the deflagration. Since each entry represents the results of a one-time-only calculation of the steady state propagation of a flame under a condition representative of the flow field under consideration, the details used in achieving each entry can be as comprehensive as desired. No additional effort is expended for such details once the dictionary has been compiled. The dictionary totally eliminates the need of continually performing the costly and arduous tasks of calculating the progress of the flame and the details of the flame structure at each instant in time.

Numerical experiments indicate that the temperature distributions, flame burning speeds, and flame trajectories calculated by the dictionary technique agree extremely well with those obtained by the

finite-difference technique. The major advantage of the dictionary technique is that grid spacings several orders of magnitude greater than those required by conventional finite-difference techniques can be used and provide exactly the same results. The progress of the deflagration within this crude mesh is governed by the details of the flame process based on calculations using a subcritical grid spacing. Such a contraction in grid-point requirements makes the problem of modeling combustion in devices of current interest feasible.

Numerical experiments also indicated that the effects of neglecting heat transfer in the non-reacting portions of the flow field are negligible. Elimination of heat transfer calculations allows the dictionary technique to be coupled to grid-free techniques. Chorin's techniques account for the fluid behavior in the boundary layer as well as in the inviscid core [2]. Accounting for turbulence in the flow field and the extention to 2 or 3 dimensions with irregular boundaries is a straightforward extension of the one dimensional method [1,3,5]. The wrinkling of the flame front due to turbulent mixing is handled by Chorin's [4] flame advection and propagation algoritms.

Two major premises must be met to successfully apply the dictionary technique in reactive gas flows: (1) the combustion event can be treated as a deflagration in the flow field, and (2) the characteristic time for flame adjustment to disturbances in the flow field is shorter than the characteristic time between encountering such disturbances. The latter restriction allows the instantaneous

state of the flame to be approximated by its steady-state conditions. Both these premises are generally satisfied whenever the flow field and the disturbance within it are at least an order of magnitude larger than the flame thickness. Combustion within the fluid boundary layer of a wall does not satisfy these two premises and so, requires either conventional techniques or the development of other techniques for their solution. The effect of mutual interaction of flame fronts which have been folded into a cusp on (a) the burning speed, and (b) other flame properties also requires further study.

It is the author's hope that the dictionary technique will further the use of numerical simulation as a design tool and/or as a means of analysis of practical reactive gas flows of current interest.

ACKNOWLEDGMENT

The author gratefully acknowledges the contribution of Alexandre Chorin in all phases of this paper. This work was supported by the Physics, Computer Science and Mathematics Division of the U. S. Department of Energy under contract No. W-7405-ENG-48.

REFERENCES

1. A. J. Chorin, J. Computational Phys. 22 (1976), 517.
2. A. J. Chorin, J. Computational Phys. 27 (1978), 428.
3. A. J. Chorin, Lawrence Berkeley Laboratory Preprint 8333, 1978, to appear in SIAM Journal on Scientific and Statistical Comp.
4. A. J. Chorin, Lawrence Berkeley Laboratory Preprint 8826, 1978, to appear in J. Computational Phys.
5. G. A. Sod, Lawrence Bekeley Laboratory Preprint 9049, 1979, to appear in J. Computational Phys.
6. F. A. Williams, "Combustion Theory," Addison-Wesley, Reading/Palo Alto, 1965.
7. A. K. Oppenheim, "Introduction to Gasdynamics of Explosions," Springer-Verlag, New York, 1972.
8. R. E. Weston, Jr. and H. A. Schwarz, "Chemical Kinetics," Prentice-Hall, Englewood Cliffs, 1972.
9. R. A. Strehlow, "Fundamentals of Combustion," International Textbook Co., Scranton, 1968.
10. W. G. Vincenti and C. H. Kruger, "Introduction to Physical Gas Dynamics," John Wiley and Sons, New York, 1965.
11. H. A. Dwyer and B. R. Sanders, Acta Astronautica 5 (1978), 1171.
12. C. W. Gear, "Numerical Initial Value Problems in Ordinary Differential Equations," Prentice-Hall, Englewood Cliffs, 1971.
13. A. C. Hindmarsh, Lawrence Livermore Laboratory, UCLR-51186, March 20, 1972.

14. R. D. Richtmyer and K. W. Morton, "Difference Methods for Initial Value Problems," Interscience, New York, 1967.

15. N. N. Yanenko, "The Method of Fractional Steps," Springer-Verlag, New York, 1971.

16. I. Karasalo, private communication, Lawrence Berkeley Laboratory, 1979.

17. J. Kurylo, Lawrence Berkeley Laboratory Preprint 9135, 1979.

TABLE I.
Calculated and predicted flame properties for various values of the model equations' parameters.

S_{calc}	S_{pred}	δ_{calc}	δ_{pred}	N_{Da_o}	K_o (sec^{-1})	σ (cm^2/sec)	T_o	T_u
331.1	337.7	0.0332	0.0335	6.140×10^4	92,103	1.50	0.500	0.150
466.9	477.6	0.0235	0.0237	1.228×10^5		0.75		
98.3	100.3	0.1120	0.1127	5.418×10^3		17.0		
233.7	238.8	0.0471	0.0474	3.070×10^4	46,052			
467.1	477.5	0.0243	0.0237	1.228×10^5	184,207			
196.1	202.3	0.0324	0.0324				0.750	
485.7	495.6	0.0409	0.0414				0.350	
485.7	495.6	0.0408	0.0414					0.300

TABLE II

Contents of the flame dictionary

entry number i	T_i	S_{u_i}	δ_i
1	0.150	313.7	0.0322
2	0.200	352.9	0.0349
3	0.250	398.0	0.0367
4	0.300	454.1	0.0398
5	0.350	535.3	0.0446
6	0.400	668.0	0.0530
7	0.450	939.5	0.0722

FIGURE CAPTIONS

Fig. 1. Heat release rates for a well-stirred reactor (WSR), Arrhenius kinetic expression, and Eq. (4).

Fig. 2. The effect of grid spacing on the flame burning speed and flame thickness.

Fig. 3. Temperature distribution within the flame for various grid spacings.

Fig. 4a. Temperature distribution within the flame for various upstream temperatures - T_u.

Fig. 4b. Progress parameter distribution within the flame for various upstream temperatures - T_u.

Fig. 5. Flow field temperature distributions calculated by the finite-difference method [$|x|$ - flame location and flame width calculated by the dictionary technique ($\sigma = 0$)].

Fig. 6. Flow field temperature distributions calculated by the dictionary technique ($\sigma = 1.5$).

Fig. 7. Flow field temperature distributions calculated by the dictionary technique ($\sigma = 0$).

Fig. 8. Flame burning speed-space profiles and flame trajectories calculated by the finite difference method (——) and the dictionary techniques with $\sigma = 0$ (- - -) and $\sigma = 1.5$(o).

Fig. 9. Flow field temperature distributions calculated by the finite-difference method and the dictionary technique ($\sigma = 1.5$) [$|x|$ - flame location and flame width calculated by the dictionary technique ($\sigma = 0$)].

Fig. 10. Flame burning speed-space profiles and flame trajectories calculated by the finite difference method (——) and the dictionary technique with $\sigma=0$ (- - -) and $\sigma = 1.5$(o).

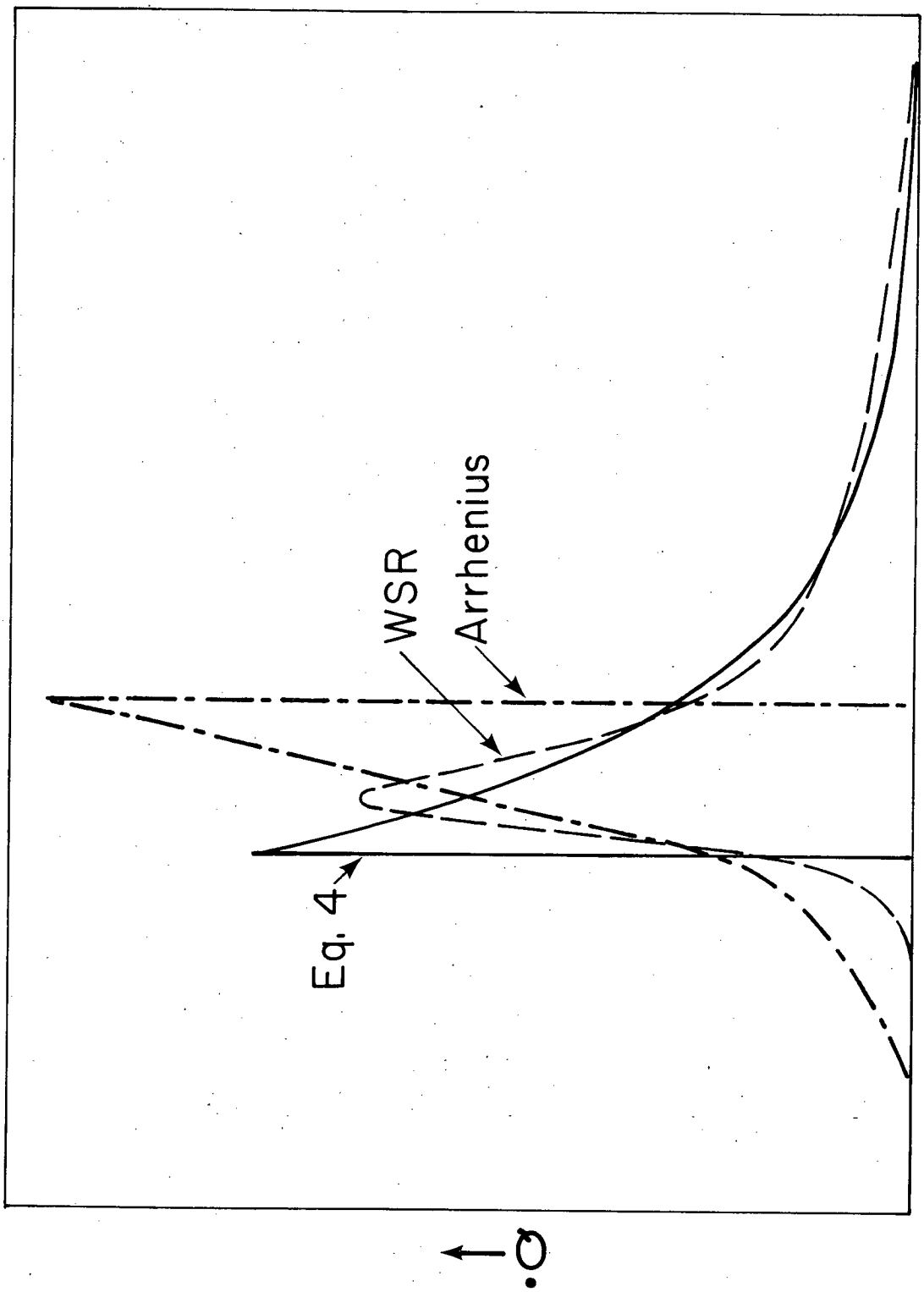

XBL 798-2514

Fig. 1

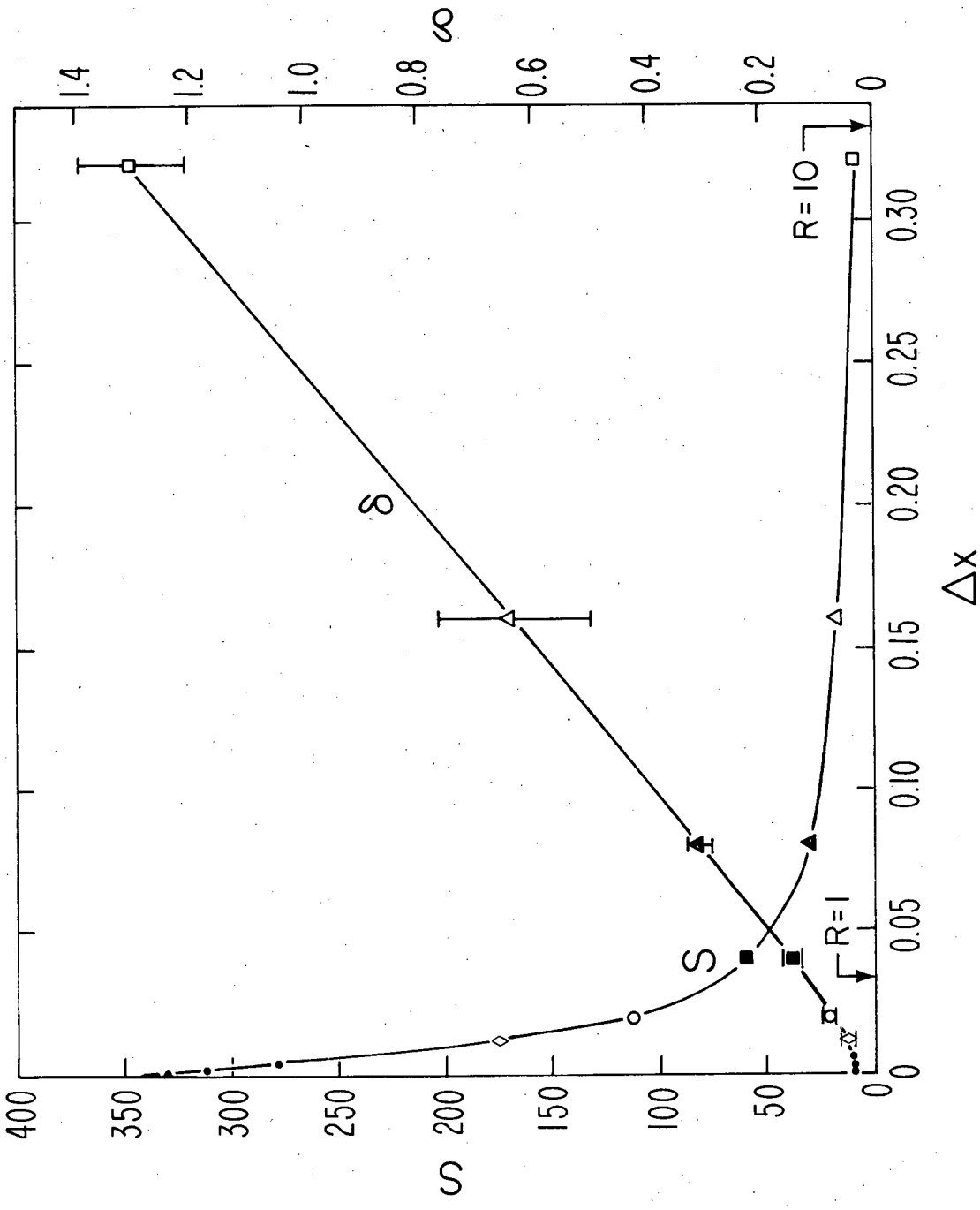

XBL798-2515

Fig. 2

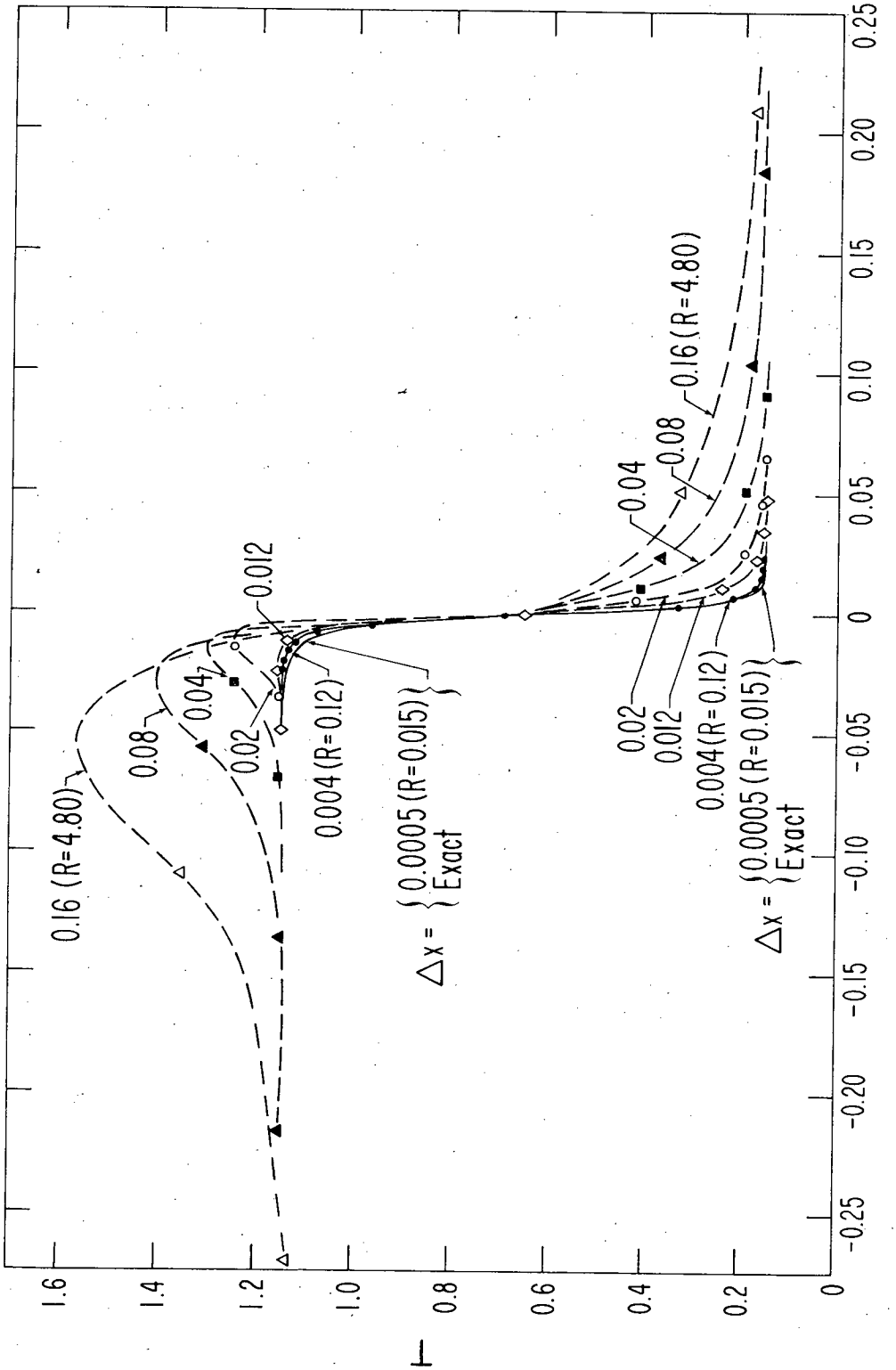

XBL 798-2516

Fig. 3

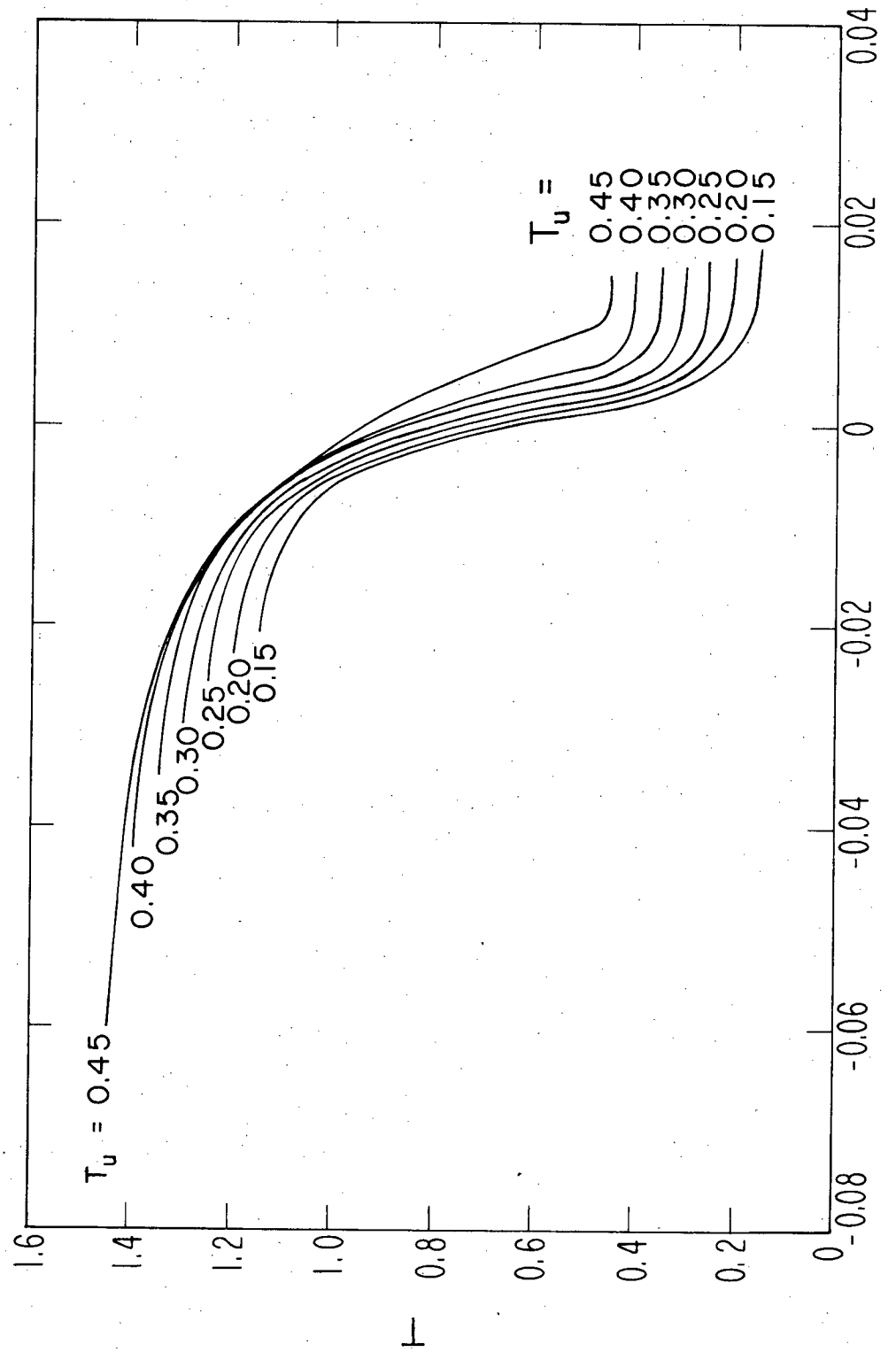

XBL 798-2517

Fig. 4a

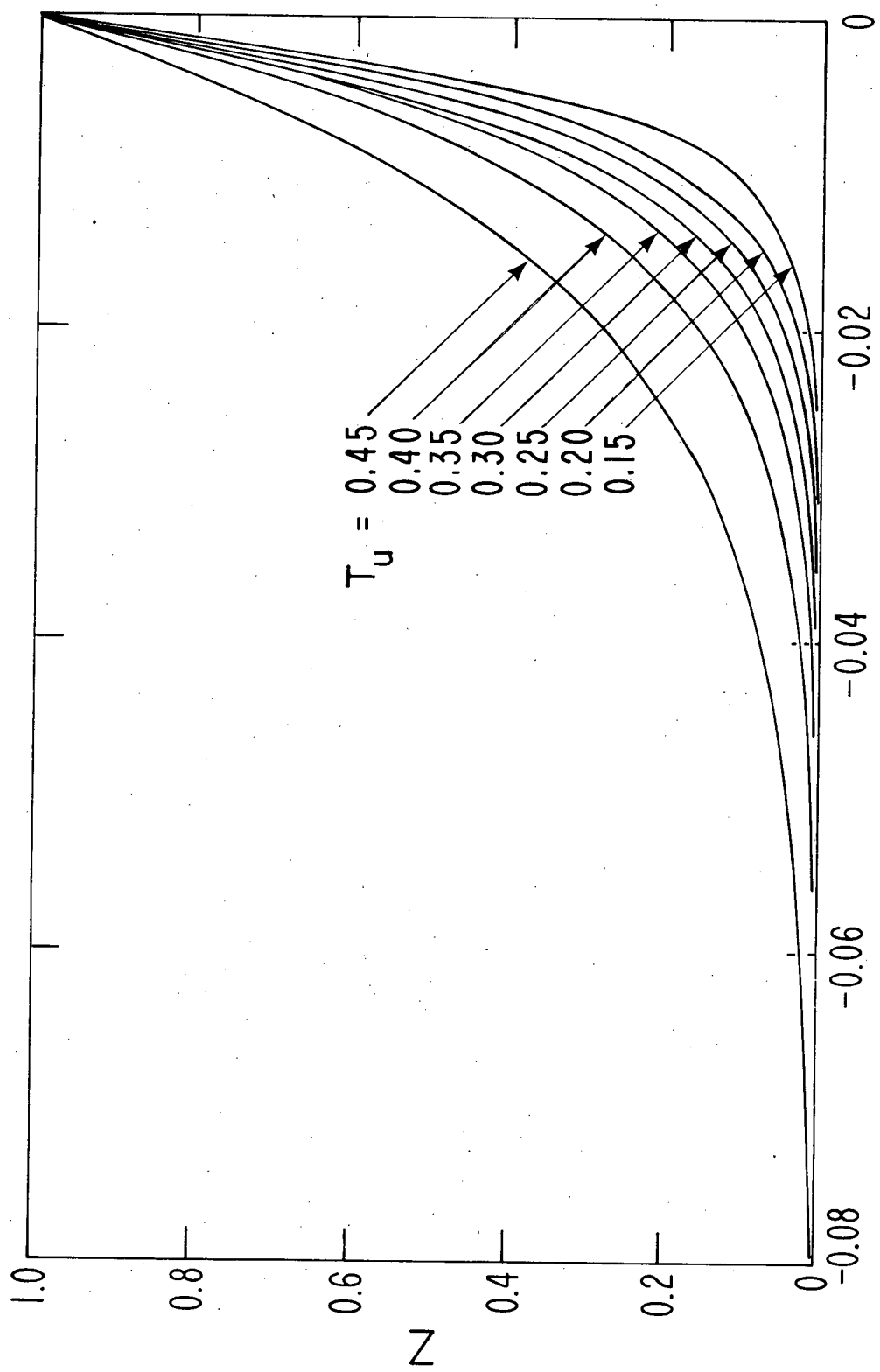

XBL 798-2518

Fig. 4b

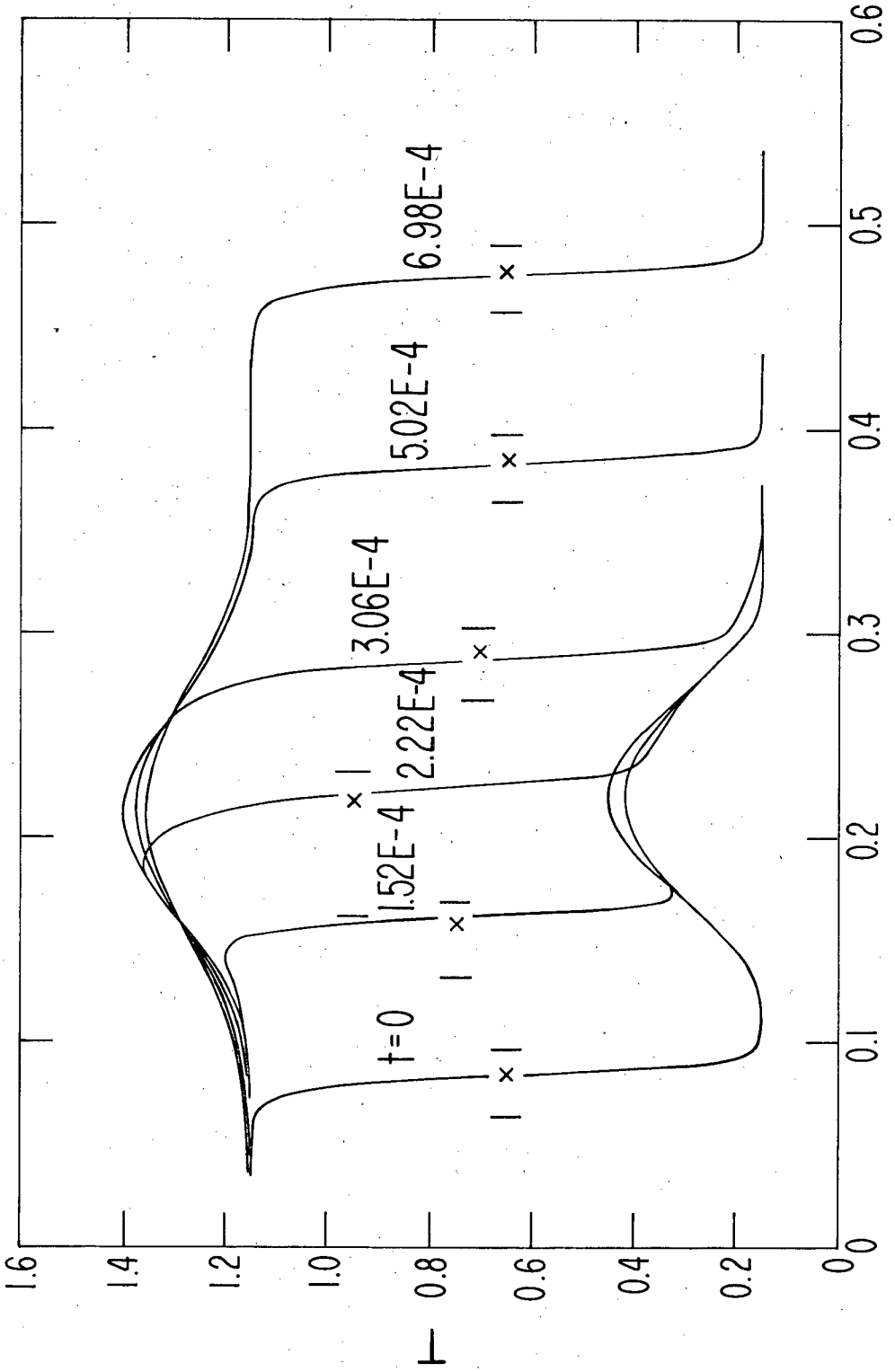

XBL 798-2521

Fig. 5

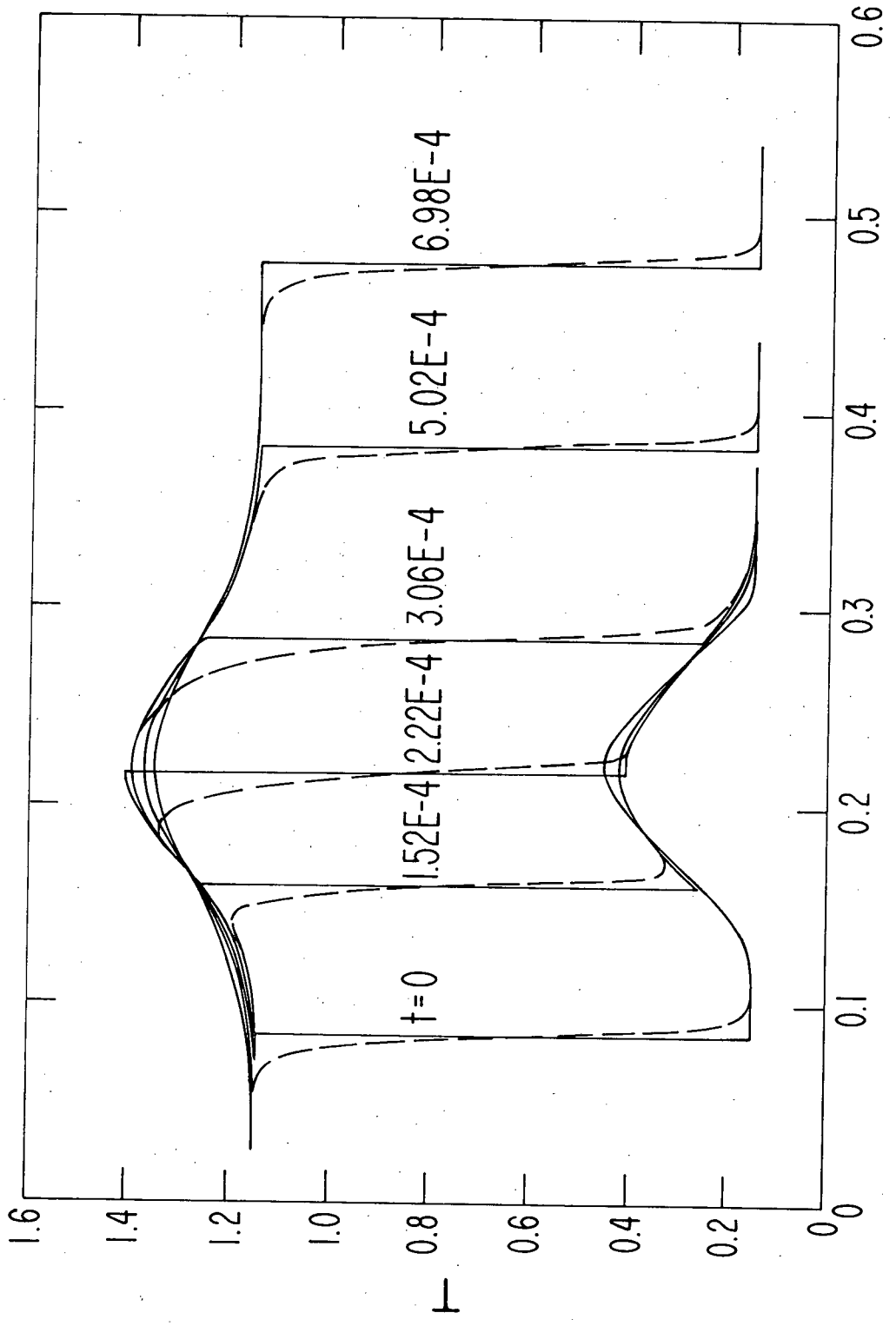

XBL798-2522

Fig. 6

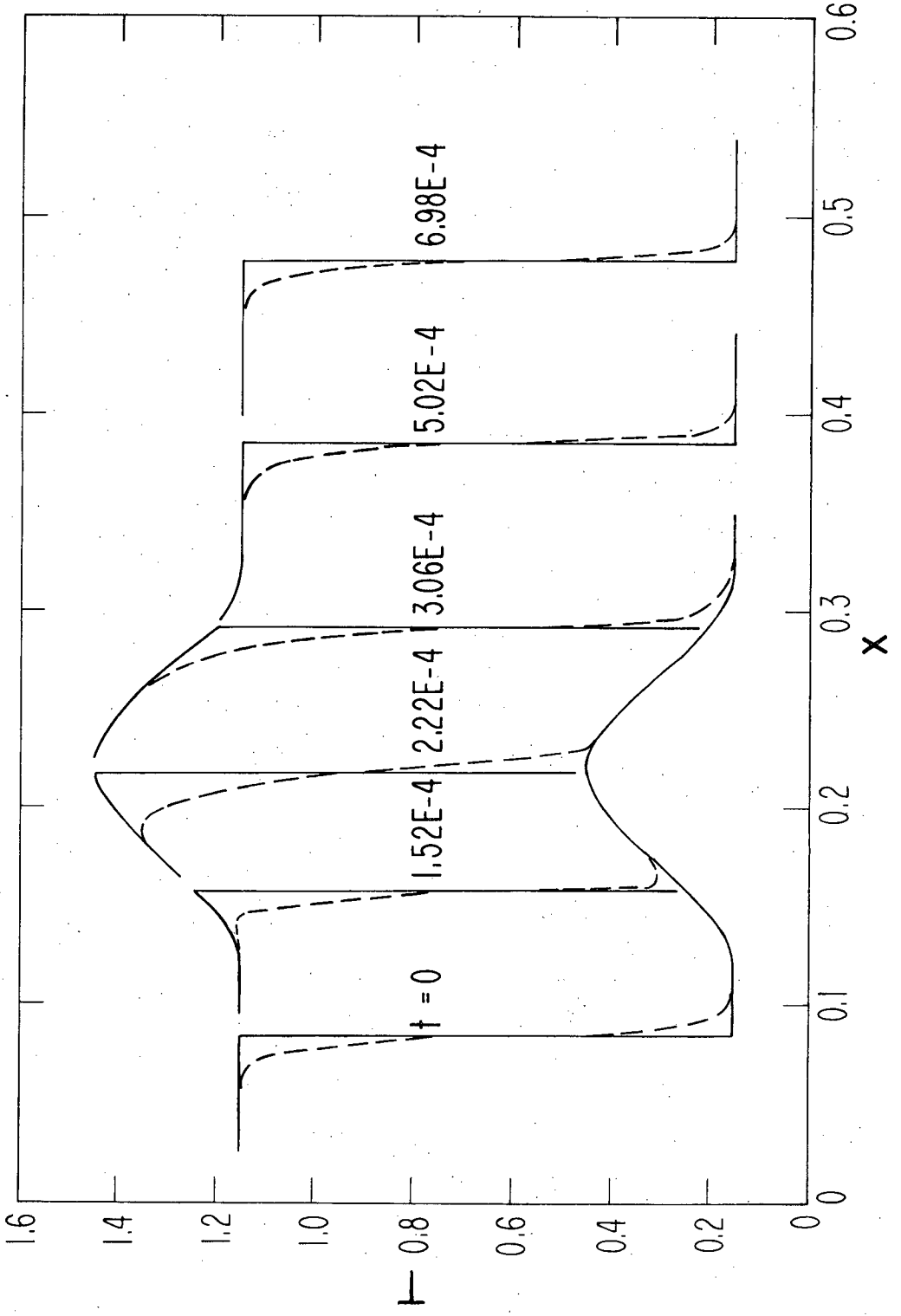

XBL 798-2519

Fig. 7

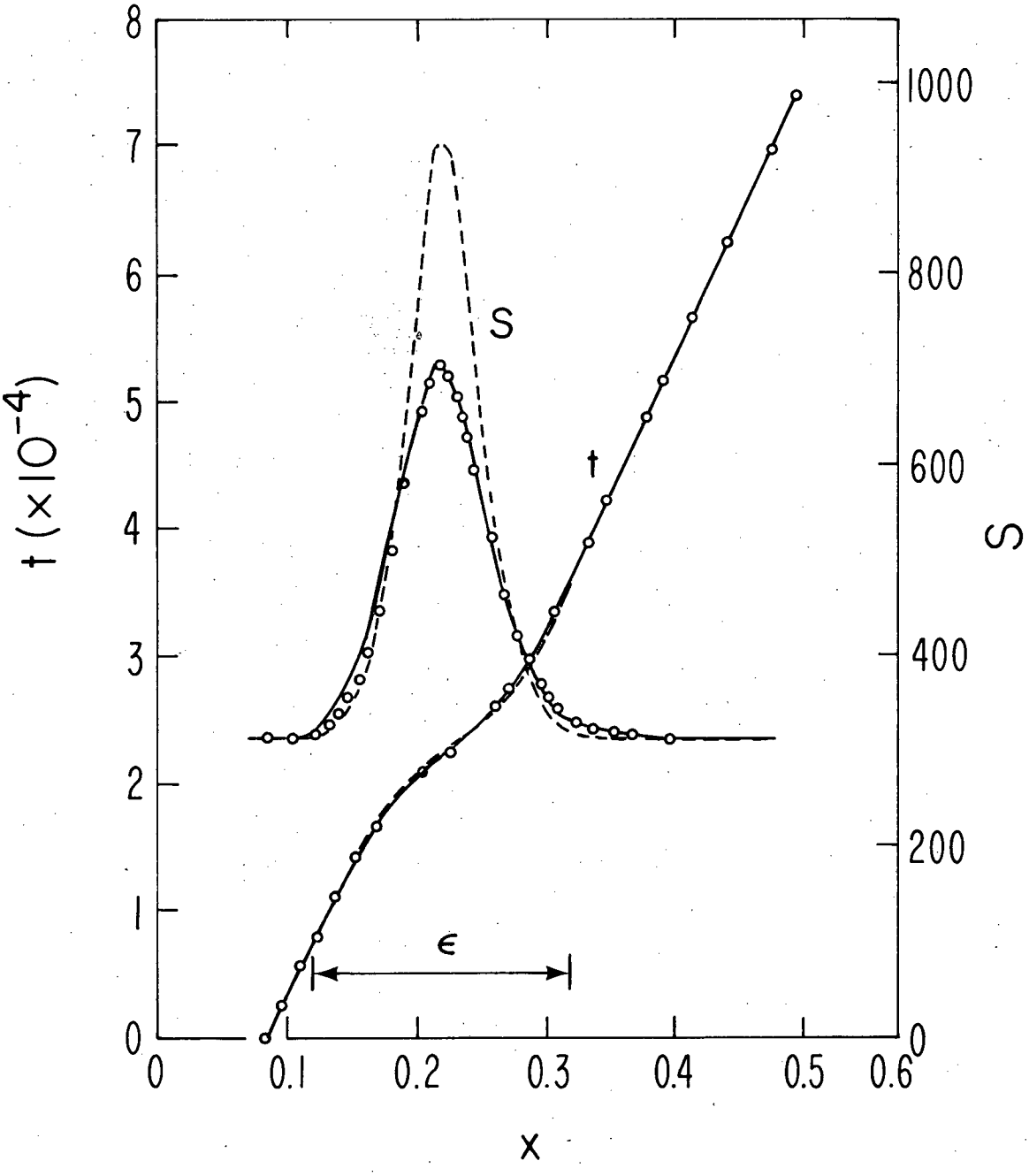

Fig. 8

XBL 798-2718

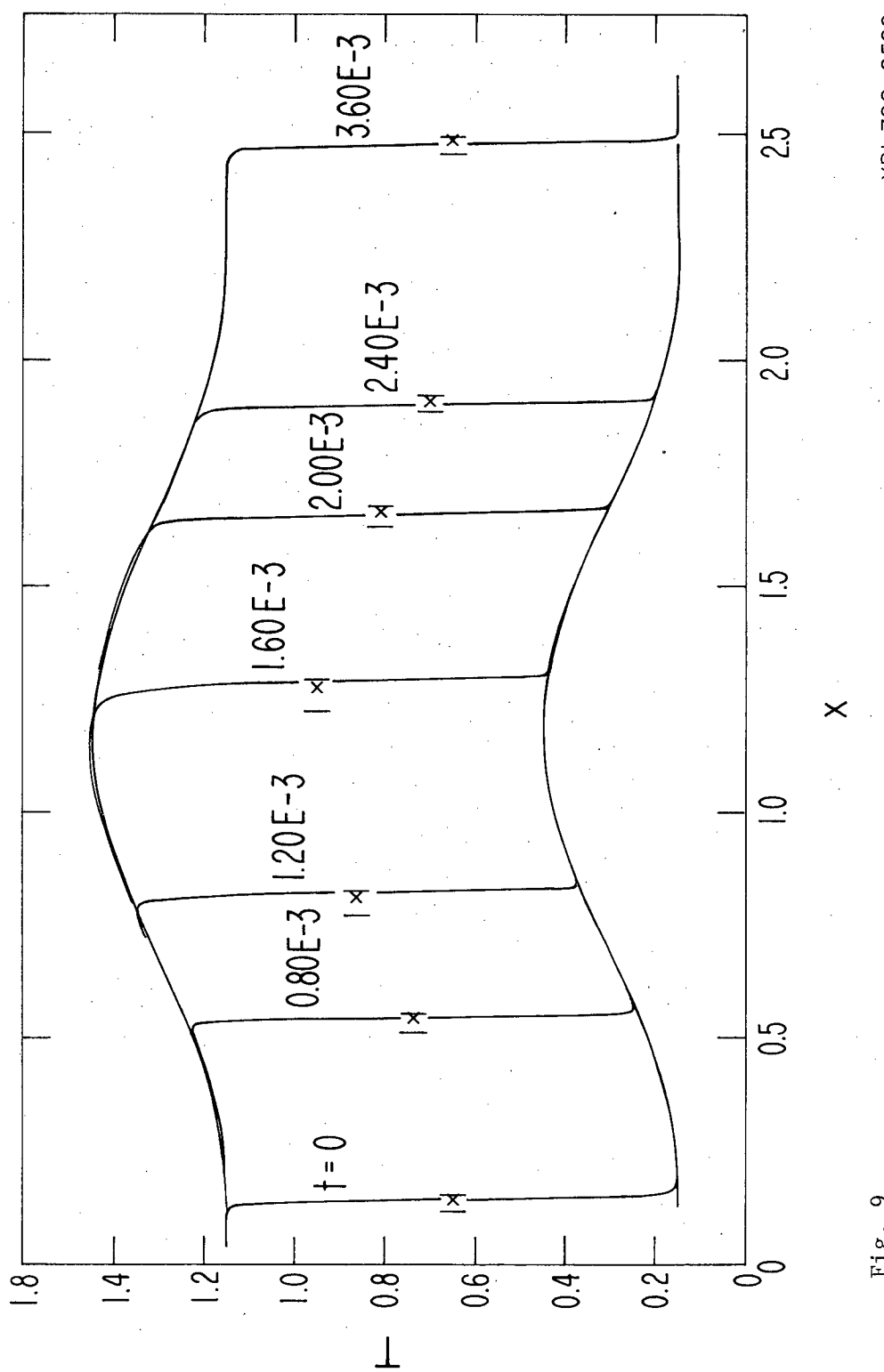

XBL 798-2520

Fig. 9

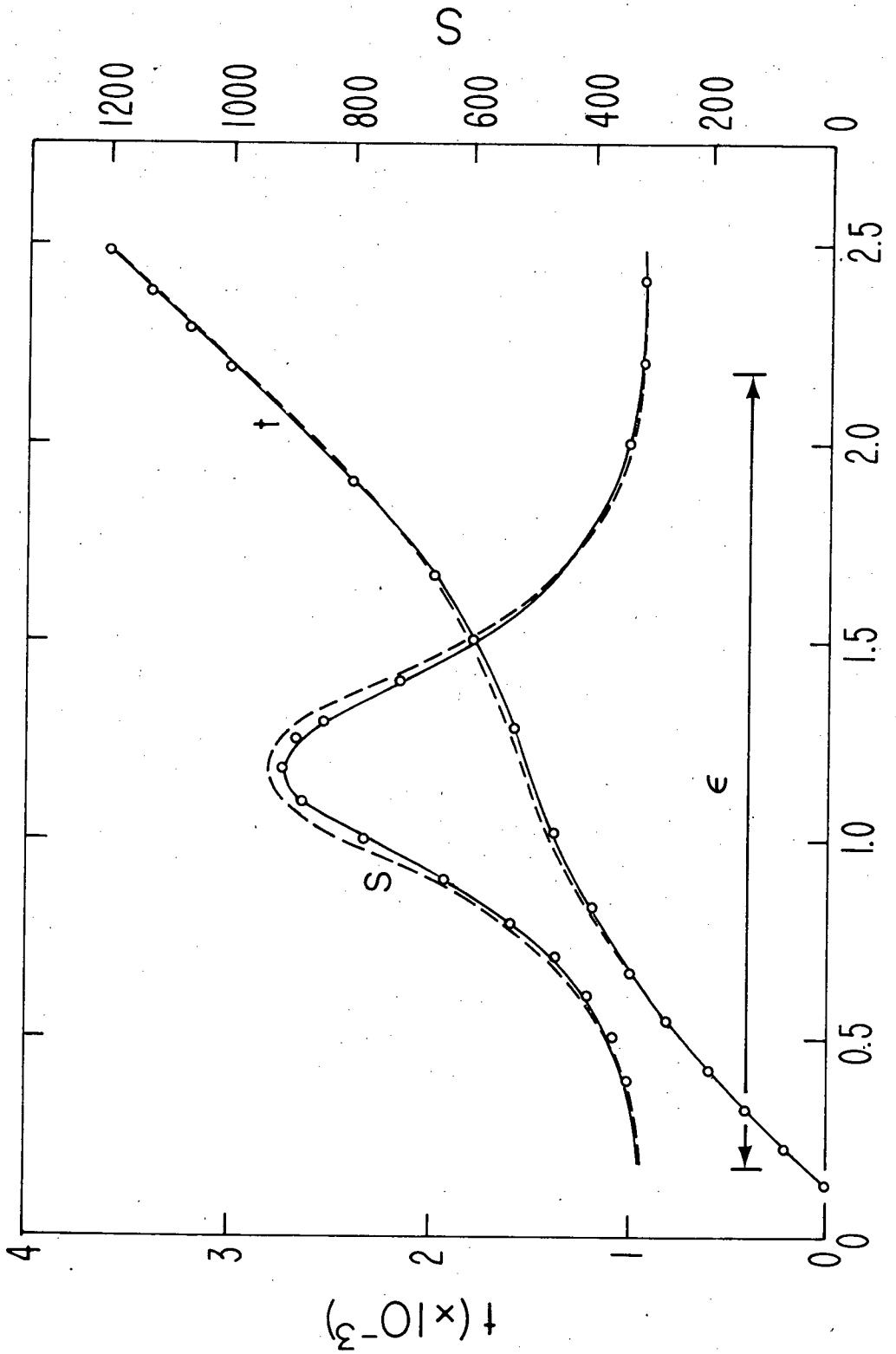

XBL 798-2523

Fig. 10

TECHNICAL INFORMATION DEPARTMENT
LAWRENCE BERKELEY LABORATORY
UNIVERSITY OF CALIFORNIA
BERKELEY, CALIFORNIA 94720